(1), Figure 2 presents a low-temperature ^{13}C NMR spectrum of 1, Figure 3 shows a cyclic voltammogram of 1, Figure 4 shows the two relative orientations of the disordered toluene molecule found in the solid-state structure of 1·tol, tables of idealized coordinates for the hydrogen atoms and thermal parameters for all atoms for 1·tol (6 pages); a listing of the observed and calculated structure factor amplitudes for 1·tol (20 pages). Ordering information is given on any current masthead page.

Molybdenum-Promoted Nitrosyl Bond Activation: Synthesis and Characterization of $(\eta^5\text{-}C_5Me_5)_3Mo_3Co_2(CO)_8(\mu_3\text{-}NH)(\mu_4\text{-}N)$, an Unusual Mixed-Metal Cluster Containing Tetrametal-Coordinated Nitrido and Trimetal-Coordinated Imido Ligands, and of $(\eta^5\text{-}C_5Me_5)_2Mo_2Co_3(CO)_{10}(\mu_5\text{-}N)$, a 74-Electron Square-Pyramidal Mixed-Metal Cluster Containing a Pentametal-Coordinated Nitrido Ligand

Charles P. Gibson[1] and Lawrence F. Dahl*

Department of Chemistry, University of Wisconsin—Madison, Madison, Wisconsin 53706

Received September 15, 1986

An attempt to provide a new synthetic route to ON-capped metal clusters (which are relatively rare) via cycloaddition of a photolytically generated metal nitrosyl fragment to the Mo–Mo triple-bonded $Mo_2(\eta^5\text{-}C_5Me_5)_2(CO)_4$ dimer has led instead to Mo-promoted N–O bond cleavage to give two unusual nitrido-containing metal clusters—viz., $(\eta^5\text{-}C_5Me_5)_3Mo_3Co_2(CO)_8(\mu_3\text{-}NH)(\mu_4\text{-}N)$ (1) as a major mixed-metal product (11% yield) and $(\eta^5\text{-}C_5Me_5)_2Mo_2Co_3(CO)_{10}(\mu_5\text{-}N)$ (2) as a minor product (<1% yield). Other major products from the photolytic reaction of $Co(CO)_3NO$ with the 30-electron $Mo_2(\eta^5\text{-}C_5Me_5)_2(CO)_4$ in THF were $Mo(\eta^5\text{-}C_5Me_5)(CO)_2NO$ and $Mo_2(\eta^5\text{-}C_5Me_5)_2(CO)_6$. Elemental, spectroscopic (IR and ^1H and ^{15}N NMR), and single-crystal X-ray diffraction analyses established that 1 possesses a butterfly $Mo_2Co_2(\mu_4\text{-}N)$ core composed of two backbone Co and two wingtip Mo atoms coordinated to a five-electron-donating N atom. This "edge-opened" tetrahedral metal fragment may be viewed as an electron-precise, 62-electron system in which the Co and Mo atoms of one bonding Co–Mo edge are each linked by additional electron-pair bonds to the Mo and N atoms of a five-electron-donating $Mo(\eta^5\text{-}C_5Me_5)(CO)_2NH$ fragment. The edge-fusion of the resulting "closed" tetrahedral $Mo_2Co(\mu_3\text{-}NH)$ system to the central butterfly $Mo_2Co_2(\mu_4\text{-}N)$ core produces an overall $Mo_3Co_2(\mu_3\text{-}NH)(\mu_4\text{-}N)$ cluster which is encapsulated by three Mo-coordinated C_5Me_5 and eight carbonyl ligands. A crystallographic characterization of 2 revealed a central $Mo_2Co_3(\mu_5\text{-}N)$ core whose idealized C_{2v} geometry consists of a square-pyramidal Mo_2Co_3 architecture containing a pentametal-coordinated (five-electron-donating) nitrido ligand positioned slightly below the basal Mo_2Co_2 plane. Inclusion of the two Mo-coordinated C_5Me_5 ligands and ten carbonyl groups (three of which are doubly bridging) lowers the symmetry to the crystallographically imposed molecular mirror plane which passes through the apical Co and two basal Co atoms, the nitride atom, and one bridging and three terminal carbonyl groups. This 74-electron square-pyramidal metal cluster is electronically equivalent and structurally analogous to the prototype carbido cluster, $Fe_5(CO)_{15}(\mu_5\text{-}C)$, and the corresponding nitrido cluster, $Fe_5(CO)_{14}(\mu_2\text{-}H)(\mu_5\text{-}N)$. $(\eta^5\text{-}C_5Me_5)_3Mo_3Co_2(CO)_8(\mu_3\text{-}NH)(\mu_4\text{-}N)$ (1): recrystallized from CH_2Cl_2/hexane with one dichloromethane molecule of crystallization ($1\cdot CH_2Cl_2$); triclinic; $P\bar{1}$; $a = 12.066$ (1) Å, $b = 13.683$ (1) Å, $c = 15.410$ (1) Å, $\alpha = 85.781$ (2)°, $\beta = 80.245$ (6)°, $\gamma = 69.060$ (6)°, $V = 2342$ Å^3 at $T = 295$ K; $d_{obsd} = 1.62$ g/cm^3 vs $d_{calcd} = 1.64$ g/cm^3 for $Z = 2$; least-squares refinement for one independent $1\cdot CH_2Cl_2$ converged at $R_1(F) = 5.43\%$ and $R_2(F) = 8.23\%$ for 4369 independent data ($I > 3\sigma(I)$) and 286 variables. $(\eta^5\text{-}C_5Me_5)_2Mo_2Co_3(CO)_{10}(\mu_5\text{-}N)$ (2): recrystallized from hexane with one C_6H_{14} molecule of crystallization (2·hex); orthorhombic; $Cmc2_1$; $a = 14.770$ (2) Å, $b = 28.846$ (10) Å, $c = 9.357$ (2) Å, $V = 3987$ Å^3 at $T = 295$ K; $d_{calcd} = 1.61$ g/cm^3 for $Z = 4$; least-squares refinement for the independent one-half molecule converged at $R_1(F) = 3.76\%$ and $R_2(F) = 4.05\%$ for 1875 independent data ($I > 3\sigma(I)$) and 167 parameters.

Introduction

The synthesis of organometallic clusters via the cycloaddition of coordinatively unsaturated organometallic carbonyl fragments to ethylene-like organometallic dimers has been shown to be a broadly applicable, rational approach for obtaining new trimetallic cluster compounds.[2] The utility of this synthetic pathway has prompted us to investigate similar additions to the inorganic acetylene analogue, $Mo_2(\eta^5\text{-}C_5Me_5)_2(CO)_4$ (3).[3] Recently, we have reported the initial results of several reactions of 3 with metal carbonyl fragments which have led to the isolation of new tri- and tetrametallic mixed-metal clusters.[4-7] Because of our interest in the preparation and examination of the physicochemical behavior of nitrosyl-capped metal clusters (only a few of which have been isolated and characterized[8]), we sought to further extend this synthetic approach to include the addition of organometallic nitrosyl fragments to 3.

An attractive feature of metal carbonyl–nitrosyl complexes is that they can be photolytically activated to more than one reactive species. For example, photolysis of the 18-electron $Co(CO)_3NO$ molecule (4) could lead to (1) a metal-to-ligand charge-transfer photoprocess[9-12] with

---

[1] Based, in part, on the Ph.D. Thesis of C.P. Gibson, University of Wisconsin—Madison, 1985. Present address: Department of Chemistry, West Virginia University, Morgantown, WV 26506.

0276-7333/88/2307-0543$01.50/0

formation of the "excited-state" 16-electron $Co(CO)_3NO$ species (**4a**) possessing a one-electron-donating "bent" nitrosyl ligand and/or (2) loss of a carbonyl group to give the 16-electron $Co(CO)_2NO$ species (**4b**) possessing an unaltered linear nitrosyl ligand.[10,11,13-19] Consequently, the cycloaddition of photoactivated **4** to the Mo–Mo triple-bonded **3** may form two different products—viz., the reaction of **3** with 4b might be expected to give a 62-electron bicyclobutane-like dimolybdenum–dicobalt nitrosyl cluster (**5**), whereas the reaction of **3** at the nucleophilic site of **4a** could result in the 48-electron ON-capped dimolybdenum–cobalt cluster (**6**).

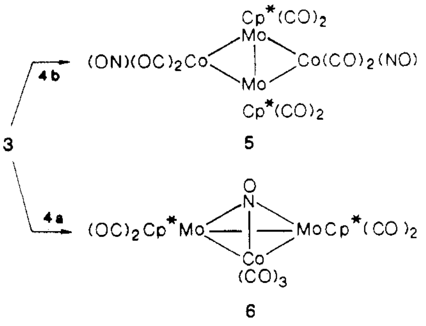

In an attempt to synthesize the unknown molybdenum–cobalt nitrosyl clusters **5** and/or **6** via the photolysis of a solution containing **3** and **4**, we unexpectedly isolated two new mixed-metal nitrido clusters—viz., $(\eta^5\text{-}C_5Me_5)_3Mo_3Co_2(CO)_8(\mu_3\text{-}NH)(\mu_4\text{-}N)$ (**1**) and $(\eta^5\text{-}C_5Me_5)_2Mo_2Co_3(CO)_{10}(\mu_5\text{-}N)$ (**2**). Herein are described the synthesis and characterization of **1**, an unusual mixed-metal cluster which contains both a tetrametal-coordinated nitrido ligand and a trimetal-coordinated imido ligand, and of **2**, a 74-electron square-pyramidal mixed-metal cluster which contains a pentametal-coordinated nitrido ligand. Both **1** and **2** are products of a reaction involving Mo-assisted cleavage of a bound nitrosyl ligand.

Experimental Section

General Procedures. All manipulations were carried out under an atmosphere of prepurified nitrogen either with a preparative vacuum line together with standard Schlenk and needle-stock techniques or within a Vacuum Atmospheres glovebox. The following solvents were freshly distilled from the indicated drying agent and then saturated with N_2 immediately prior to use: tetrahydrofuran (potassium/benzophenone), hexane (CaH_2), dichloromethane (P_2O_5), and toluene (sodium/benzophenone). Chloroform-d_1 and nitromethane were dried over activated molecular sieves and vacuum-distilled prior to use. $Mo_2(\eta^5\text{-}C_5Me_5)_2(CO)_4$ (**3**) and $Co(CO)_3NO$ (**4**) were prepared via modification of published procedures.[20,21] All other reagents were purchased from major chemical suppliers and used without further purification.

Infrared spectra were recorded on a Beckman Model 4240 spectrometer either in the solid state as a KBr disk or with 0.1-mm path-length KBr solution cells. Proton NMR spectra were obtained with either a Bruker WP-200 or a WP-270 spectrometer and were referenced indirectly to TMS via residual solvent protons. The ^{15}N NMR spectra of **1** were recorded at −70 °C with a Bruker AM-500 MHz spectrometer operated at 50.45 MHz on a sample which had been enriched to 18% ^{15}N via the synthesis of enriched **4** from 90% enriched $Na^{15}NO_2$; these ^{15}N NMR spectra were referenced indirectly to the ammonium nitrogen of NH_4NO_3 by the use of nitromethane (δ 359) as an internal standard.

Chromatographic separations were performed with Ace Glass medium-pressure chromatographic accessories which were adapted to handle air-sensitive materials. The columns were packed in hexane with neutral alumina (80–200 mesh Brockman activity III).

Preparation of $(\eta^5\text{-}C_5Me_5)_3Mo_3Co_2(CO)_8(\mu_3\text{-}NH)(\mu_4\text{-}N)\cdot CH_2Cl_2$ ($1\cdot CH_2Cl_2$). A solution containing 0.57 g (3.29 mmol) of $Co(CO)_3NO$ (**4**) and 1.80 g (3.13 mmol) of $Mo_2(\eta^5\text{-}C_5Me_5)_2(CO)_4$ (**3**) dissolved in ca. 170 mL of THF was transferred to a water-cooled Pyrex photolysis apparatus where it was irradiated with a Hanovia 450-W medium-pressure Hg vapor lamp. Throughout the course of the reaction, a slow stream of N_2 was bubbled through the solution in order to assist in mixing the solution as well as to facilitate the removal of evolved CO.

After the solution had been photolyzed for about 8 h, the contents of the reaction vessel were transferred to a 300-mL flask and the solvent was removed in vacuo. Some alumina (ca. 7 g) and THF were added to the residue, and the slurry was thoroughly mixed. the THF was then evaporated, leaving behind a dry brown powder which was carefully transferred to the top of a chromatography column containing alumina. Elution of the column with a solution of toluene in hexane (35/65 v/v) resulted in the isolation of a broad, orange-red band containing **3**, $Mo_2(\eta^5\text{-}C_5Me_5)_2(CO)_6$, and $Mo(\eta^5\text{-}C_5Me_5)(CO)_2NO$ which were identified by their characteristic infrared and ^1H NMR spectra. Subsequent elution

---

(2) See, for example: (a) Ashworth, T. V.; Howard, J. K.; Stone, F. G. A. *J. Chem. Soc., Chem. Commun.* **1979**, 42–43. (b) Cirjak, L. M.; Huang, J.-S.; Zhu, Z.-H.; Dahl, L. F. *J. Am. Chem. Soc.* **1980**, *102*, 6623–6626. (c) Green, M.; Mills, R. M.; Pain, G. N.; Stone, F. G. A.; Woodward, P. *J. Chem. Soc., Dalton Trans.* **1982**, 1309–1319. (d) Boag, N. M.; Green, M.; Mills, R. M.; Pain, G. N.; Stone, F. G. A.; Woodward, P. *J. Chem. Soc., Chem. Commun.* **1980**, 1171–1173. (e) Farrugia, L. J.; Howard, J. A. K.; Mitrprachachon, P.; Stone, F. G. A.; Woodward, P. *J. Chem. Soc., Dalton Trans.* **1981**, 155–161. (f) Farrugia, L. J.; Howard, J. A. K.; Mitrprachachon, P.; Stone, F. G. A.; Woodward, P. *J. Chem. Soc., Dalton Trans,* **1981**, 171–179. (g) Brun, P.; Dawkins, G. M.; Green, M.; Miles, A. D.; Orpen, A. G.; Stone, F. G. A. *J. Chem. Soc., Chem. Commun.* **1982**, 926–927. (h) Barr, R. D.; Green, M.; Howard, J. A. K.; Marder, T. B.; Stone, F. G. A. *J. Chem. Soc., Chem. Commun.* **1983**, 759–760. (i) Green, M.; Hankey, D. R.; Howard, J. A. K.; Louca, P.; Stone, F. G. A. *J. Chem. Soc., Chem. Commun.* **1983**, 757–758.

(3) Huang, T.-S.; Dahl, L. F. *J. Organomet. Chem.* **1983**, *243*, 57–68.

(4) Gibson, C. P.; Mahood, J. A.; Huang, J.-S.; Dahl, L. F. *Abstracts of Papers*, 187th National Meeting of the American Chemical Society, St. Louis, MO; American Chemical Society: Washington, DC, 1984; INOR 202.

(5) Gibson, C. P.; Huang, J.-S.; Dahl, L. F. *Organometallics* **1986**, *5*, 1676–1681 and references cited therein.

(6) (a) Mahood, J. A.; Gibson, C. P.; Dahl, L. F. *Abstracts of Papers*, 190th National Meeting of the American Chemical Society, Chicago, IL; American Chemical Society: Washington, DC, 1985; INOR 77. (b) Gibson, C. P.; Adams, B. R.; Dahl, L. F. *Abstracts of Papers*, 190th National Meeting of the American Chemical Society, Chicago, IL; American Chemical Society: Washington, DC, 1985; INOR 73.

(7) Gibson, C. P.; Dahl, L. F. *Organometallics*, preceding paper in this issue.

(8) The few known metal clusters containing a triply bridging nitrosyl ligand include (a) $Mn_3(\eta^5\text{-}C_5H_5)_3(\mu_2\text{-}NO)_3(\mu_3\text{-}NO)$: Elder, R. C. *Inorg. Chem.* **1974**, *13*, 1037–1042. (b) $Mn_3(\eta^5\text{-}C_5H_4Me)_3(\mu_2\text{-}NO)_3(\mu_3\text{-}NO)$: Kolthammer, B. W. S.; Legzdins, P. *J. Chem. Soc., Dalton Trans.* **1978**, 31–35. (c) $Co_3(\eta^5\text{-}C_5H_5)_3(\mu_3\text{-}NO)_2$: Müller, J.; Schmitt, S. *J. Organomet. Chem.* **1975**, *97*, C54–C56. (d) $Co_3(\eta^5\text{-}C_5H_4Me)_3(\mu_3\text{-}NO)_2$: Kubat-Martin, K. A.; Rae, A. D.; Dahl, L. F. *Organometallics* **1985**, *4*, 2221–2223. (e) $Rh_3(\eta^5\text{-}C_5H_5)_3(\mu_3\text{-}NO)_2$: Dimas, P. A.; Lawson, R. J.; Shapley, J. R. *Inorg. Chem.* 1981, *20*, 281–283. (f) $[Co_3(\eta^5\text{-}C_5H_{5-x}Me_x)_3(\mu_3\text{-}NH)(\mu_3\text{-}NO)]^n$ (x = 0.1; n = 1+, 0): Bedard, R. L.; Dahl, L. F. *J. Am. Chem. Soc.* **1986**, *108*, 5942–5948. (g) $[(\eta^5\text{-}C_5H_4Me)MnFe_2(\eta^5\text{-}C_5H_5)_2(\mu_2\text{-}CO)_2(\mu_2\text{-}NO)(\mu_3\text{-}NO)]^n$ (n = 0, 1−): Kubat-Martin, K. A.; Spencer, B.; Dahl, L. F. *Organometallics* **1987**, *6*, 2580–2587.

(9) Liu, P. H.; Zink, J. I. *Inorg. Chem.* **1977**, *16*, 3165–3170.

(10) Crichton, O.; Rest, A. J. *J. Chem. Soc., Dalton Trans.* **1978**, 208–215.

(11) Crichton, O.; Rest, A. J. *J. Chem. Soc., Dalton Trans.* **1978**, 202–207.

(12) Evans, W.; Zink, J. I. *J. Am. Chem. Soc.* **1981**, *103*, 2635–2640.

(13) Treichel, P. M.; Pitcher, E.; King, R. B.; Stone, F. G. A. *J. Am. Chem. Soc.* 1961, *33*, 2593–2594.

(14) Keeton, D. P.; Basolo, F. *Inorg. Chim. Acta* **1972**, *6*, 33–38.

(15) Crichton, O.; Rest, A. J. *J. Chem. Soc., Dalton Trans.* **1977**, 986–993.

(16) Clark, R. J. *Inorg. Chem.* **1967**, *6*, 299–303.

(17) Sabherwal, I. H.; Burg, A. *J. Chem. Soc. D* **1969**, 853–854.

(18) Crichton, O.; Rest, A. J. *J. Chem. Soc., Dalton Trans.* **1977**, 536–541.

(19) Crichton, O.; Rest, A. J. *J. Chem. Soc., Dalton Trans.* **1977**, 656–661.

(20) Job, R.; Rovang, J. *Synth. React. Inorg. Met.-Org. Chem.* **1976**, *6*, 367–371.

(21) King, R. B.; Iqbal, M. Z.; King, A. D., Jr. *J. Organomet. Chem.* **1979**, *171*, 53–63.

with copious amounts of toluene brought down a very broad, brown band containing **1** and several other minor species which have not been identified. The solvent was evaporated from this band with a stream of N_2, and the residual brown material was dried in vacuo. This material was extracted with several small portions of benzene; careful layering of hexane over the combined benzene extracts resulted in the precipitation of black microcrystals. This material was recrystallized from a hexane-CH_2Cl_2 mixture to give 100–400 mg (0.09–0.36 mmol, 3–11%) of $\mathbf{1}\cdot CH_2Cl_2$ as black crystals. Alternatively, **1** can be separated from the reaction products (with considerably more difficulty) via solvent extractions. Anal. Calcd for $C_{39}H_{48}N_2O_8Mo_3Co_2Cl_2$: C, 40.75; H, 4.21; N, 2.44. Found: C, 39.15; H, 4.40; N, 2.29. An experimental density of 1.62 ± 0.03 g/cm^3 was obtained by the flotation method.

Proton NMR spectra of $\mathbf{1}\cdot CH_2Cl_2$ exhibited resonances at δ 1.83 (s, 15 H), 1.88 (s, 15 H), 1.95 (s, 15 H), and 5.32 (s, 2 H) in $CDCl_3$. No ^{1}H NMR resonance could be assigned to the imido hydrogen atom. ^{15}N NMR spectra of **1** contained resonances at δ 518 (s, 1 N) and 190 (d, 1 N, $J(^1H-^{15}N) = 76$ Hz). The peak at δ 518 was assigned to the μ_4-N nitrogen atom, while the doublet centered at δ 190 was assigned to the μ_3-imido nitrogen atom.

An infrared solid-state spectrum of **1** as a KBr disk clearly showed an absorbance at 3279 cm^{-1} which was assigned to the imido N–H stretching mode. A solution infrared spectrum of **1** (CH_2Cl_2) exhibited bands in the carbonyl stretching region at 2003 (s), 1974 (s), 1860 (s), 1838 (m), and 1770 (w) cm^{-1}.

Preparation of $(\eta^5\text{-}C_5Me_5)_2Mo_2Co_3(CO)_{10}(\mu_5\text{-}N)\cdot C_6H_{14}$ (2·hex). A solution of **3** and **4** was photolyzed as described in the preceding section. The contents of the photolysis unit were transferred to a 300-mL flask where removal of the solvent in vacuo gave a brown tar. This brown residue was extracted with several small portions of dichloromethane, and the combined extracts were carefully loaded onto a column containing alumina. Elution of the column with hexane brought down an orange band containing $Mo(\eta^5\text{-}C_5Me_5)(CO)_2NO$ as the major component. The solvent was removed from this material, and the reddish orange solid was dried in vacuo. This material was then extracted with several small portions of *n*-hexane, and the combined extracts were transferred to a small test tube which was sealed in a wide Schlenk tube containing decane. After equilibration for about 2 weeks, most of the solvent from the inner tube had evaporated, leaving behind a large number of well-formed orange crystals of $Mo(\eta^5\text{-}C_5Me_5)(CO)_2NO$ together with several small needles of **2·hex** which were separated manually and subsequently characterized by X-ray crystallography.

Investigation of Possible Reactions of $Mo(\eta^5\text{-}C_5Me_5)(CO)_2NO$ with Either $Mo_2(\eta^5\text{-}C_5Me_5)_2(CO)_4$ or $Co(CO)_3NO$. Infrared spectra that were recorded during the course of the photolytic reaction between $Mo_2(\eta^5\text{-}C_5Me_5)_2(CO)_4$ (**3**) and $Co(CO)_3NO$ (**4**) in THF revealed that the major product, $Mo(\eta^5\text{-}C_5Me_5)(CO)_2NO$ (**7**), is generated in appreciable quantities rather early in course of the reaction. Since this observation raised the possibility that **7** might be reacting with either of the two starting reagents, **3** or **4**, to give isolable organometallic species (possibly including the new mixed-metal species **1** and/or **2**), several test reactions were performed.

Photolysis of a THF solution containing only **4** resulted in the decomposition of this material, as judged by the loss of carbonyl/nitrosyl stretching absorbances in an infrared spectrum of the reaction solution. Similar decomposition was noted upon photolysis of a THF solution containing only **7**, while the photolysis of a solution containing only **3** resulted in no reaction and no detectable decomposition of this material. When a THF solution containing **4** and **7** was photolyzed for 1 h, decomposition of both reagents was observed; photolysis of a THF solution containing both **3** and **7** resulted in the decomposition of only **7**.

While these reactions do not rule out the possibility that the production of **1** and **2** may require some reaction involving **7**, it is clear that under these conditions **7** does *not* react with either **3** or **4** in THF to give substantial quantities of carbonyl- or nitrosyl-containing organometallic species. However, the dramatic effect that different solvents can exert on these types of reactions is clearly illustrated in this case. If a solution consisting of both **7** and **3** in benzene or toluene is photolyzed, the compounds do react to give a trimetal-coordinated nitrido cluster, $(\eta^5\text{-}C_5Me_5)_3Mo_3(O)(CO)_4(\mu_3\text{-}N)$ (**9**), in high yield.[4,6b] Since **7** is also a major product of the reaction between **3** and **4** in benzene or toluene, significant quantities of **9** may be isolated from the reaction of **3** with **4** in benzene or toluene.

Table I. Crystal Data and Details of Data Collection and Refinement of $(\eta^5\text{-}C_5Me_5)_3Mo_3Co_2(CO)_8(\mu_3\text{-}NH)(\mu_4\text{-}N)\bullet CH_2Cl_2$

fw	1149.41
cryst system	triclinic
cell consts (23 °C)	
a, b, c (Å)	12.066 (1), 13.683 (1), 15.410 (1)
α, β, γ (deg)	85.781 (2), 80.245 (6), 69.060 (6)
V (Å^3)	2342
space group	$P\bar{1}$
Z	2
d_{calcd} (g/cm^3)	1.64
d_{obsd} (g/cm^3)	1.62
radiatn (λ, Å)	Mo K$\bar{\alpha}$ (0.71073)
μ (cm^{-1})	14.95
data-collectn temp (°C)	23
scan mode	θ–2θ
2θ limits (deg)	4.0–45.0
scan speed (deg/min)	variable (3.0–24.0)
scan width (deg above Kα_1/below Kα_2)	1.0/1.0
bkgd anal.	profile
std reflctns/freq	$\bar{2}$20, 002, 011/3 per 47
no. of data collected	6463 (four octants)
cutoff obsd data	$I_o > 3\sigma(I_o)$
no. of indep obsd data	4369
no. of parameters	286
goodness-of-fit	1.81
$R_1(F)$, $R_2(F)$ (%)	5.43, 8.23

Structural Determination of $(\eta^5\text{-}C_5Me_5)_3Mo_3Co_2(CO)_8(\mu_3\text{-}NH)(\mu_4\text{-}N)\cdot CH_2Cl_2$ ($\mathbf{1}\cdot CH_2Cl_2$). Single crystals of $\mathbf{1}\cdot CH_2Cl_2$ were grown by a careful layering of hexane over a CH_2Cl_2 solution of **1**. A parallelepiped-shaped single crystal of dimensions 0.5 × 0.3 × 0.2 mm was epoxied inside an argon-filled Lindemann glass capillary which was then hermetically sealed.

A Nicolet P$\bar{1}$ diffractometer with graphite-monochromated Mo K$\bar{\alpha}$ radiation was used to obtain intensity data at ambient temperature (23 °C). Axial photographs were used to verify the approximate dimensions of the chosen triclinic unit cell. Refined lattice constants were determined from a least-squares analysis of setting angles for 15 centered, high-angle reflections. The procedures involved in the crystal alignment and data collection are described elsewhere.[22] Specific details of this X-ray structural determination are listed in Table I. The intensities of three standard reflections did not show any significant variations (viz., <1.5%) during data collection.

Initial positions for the three molybdenum and two cobalt atoms were determined via the interpretation of a Patterson map under P$\bar{1}$ symmetry. The remaining non-hydrogen atoms of the independent cluster molecule were located from a combination of successive difference maps coupled with several cycles of isotropic least-squares refinement with RAELS.[23] At this point, each of the three independent pentamethylcyclopentadienyl ligands was constrained as a rigid group under local C_{5v} symmetry with the methyl hydrogen atoms included in their idealized positions. Both the positional parameters and thermal motion of these three groups were refined by use of subsidiary axial systems as described by Rae.[24,25]

Examination of an electron-density difference map indicated that a channel of relatively high residual electron density existed within the unit cell. The measured density of the crystals indicated that there were two dichloromethane molecules per unit cell. Their existence was verified from a resonance of the proper intensity at δ 5.32 in the ^{1}H NMR spectra of $\mathbf{1}\cdot CH_2Cl_2$. Hence, two disordered half-weighted solvent molecules (corresponding

---

(22) Byers, L. R.; Dahl, L. F. *Inorg. Chem.* **1980**, *19*, 277–284.

(23) Rae, A. D. RAELS, A Comprehensive Least-Squares Program; University of New South Wales: Kensington, 1976 adapted for a Harris/7 computer by A. D. Rae, University of Wisconsin, Madison, 1984.

(24) Rae, A. D. *Acta Crystallogr., Sect. A: Cryst. Phys., Diffr., Theor. Gen. Crystallogr.* **1975**, *A31*, 560–569.

to one independent CH_2Cl_2 molecule randomly occupying two orientations) were introduced into the refinement as rigid groups in such a way that the chlorine atoms of the solvent molecules were superimposed onto the several diffuse maxima located within the above-mentioned channel. After inclusion of positional and isotropic thermal parameters for the carbon and chlorine atoms of the disordered solvent molecules, least-squares refinement was resumed. Anisotropic thermal parameters were used for all of the atoms of 1 except for the (η^5-C_5Me_5) rings; a TLX group thermal model was used for each of these latter fragments.[25,26] During a later stage of refinement, the methyl substituents of each pentamethylcyclopentadienyl ligand were individually allowed to move away from the plane containing the ring carbon atoms. An empirical absorption correction was applied to the intensity data.[27-29] Blocked least-squares refinement converged at $R_1(F) = 5.43\%$ and $R_2(F) = 8.23\%$ with a data-to-parameter ratio of 15.2/1.[30,31] The largest parameter change-to-estimated standard deviation ratio for the final cycle was 0.23. A final difference map revealed no unusual features; the largest residual densities corresponded to several small peaks (of electron densities less than 10% of that of a typical carbon atom) located at nonmeaningful atomic sites near the molybdenum atoms.

Positional parameters for the non-hydrogen atoms from the output of the last least-squares cycle are presented in Table II. Relevant interatomic distances and bond angles for $1 \cdot CH_2Cl_2$ are listed in Table III. Tables of coordinates and isotropic temperature factors for all hydrogen atoms, anisotropic thermal parameters for all non-hydrogen atoms, and a listing of observed and calculated structure factor amplitudes are available as supplementary material.

Structural Determination of (η^5-$C_5Me_5)_2Mo_2Co_3(CO)_{10}$($\mu_5$-N)$\cdot C_6H_{14}$ (2·hex). A black uniformly-shaped needle crystal of 0.06 mm width and 0.40 mm length was attached via epoxy resin inside of an argon-filled Lindeman glass capillary which was then hermetically sealed.

A Nicolet P$\bar{1}$ diffractometer with graphite-monochromated Mo Kα radiation was used to collect intensity data at ambient temperature (23 °C). Axial photographs substantiated the approximate dimensions and mirror-plane symmetry of the chosen orthorhombic cell. Refined lattice constants were determined from a least-squares analysis of setting angles for 15 centered, high-angle reflections. The procedures involved in the crystal alignments and data collection are described elsewhere.[22] Since the intensities of the chosen standard reflections decreased by ca. 5% during data collection, a decay correction was applied. Specific details of this structural determination are listed in Table IV.

Table II. Atomic Coordinates for (η^5-$C_5Me_5)_3Mo_3Co_2(CO)_8(\mu_3$-NH)($\mu_4$-N)$\bullet CH_2Cl_2$[a]

atom	*x*	*y*	*z*
C1(S)	1.0371 (0)	0.3532 (0)	0.1711 (0)
Cl(1)	1.0346 (0)	0.3946 (0)	0.0577 (0)
Cl(2)	1.0872 (0)	0.2749 (0)	0.2116 (0)
C2(S)	0.8957 (0)	0.1390 (0)	0.0313 (0)
Cl(3)	0.7636 (0)	0.2143 (0)	0.0904 (0)
Cl(4)	0.9824 (0)	0.0508 (0)	0.1089 (0)
Mo(1)	0.2935 (1)	0.6086 (1)	0.2570 (1)
Mo(2)	0.3054 (1)	0.7476 (1)	0.3928 (1)
Mo(3)	0.5540 (1)	0.8156 (1)	0.2325 (1)
Co(1)	0.4930 (1)	0.6395 (1)	0.2877 (1)
Co(2)	0.5299 (1)	0.7354 (1)	0.4038 (1)
N(1)	0.4232 (6)	0.7883 (5)	0.3125 (5)
N(2)	0.3702 (6)	0.5929 (5)	0.3664 (4)
C(1)	0.4200 (9)	0.6299 (7)	0.1659 (6)
O(1)	0.4741 (6)	0.6329 (6)	0.0953 (4)
C(2)	0.2009 (9)	0.7530 (8)	0.2294 (7)
O(2)	0.1405 (7)	0.8327 (6)	0.1999 (5)
C(3)	0.6079 (9)	0.5144 (8)	0.2673 (6)
O(3)	0.6806 (7)	0.4341 (5)	0.2555 (5)
C(4)	0.6625 (9)	0.6238 (8)	0.4058 (7)
O(4)	0.7518 (7)	0.5577 (7)	0.4125 (6)
C(5)	0.5409 (8)	0.8232 (8)	0.4806 (7)
O(5)	0.5566 (8)	0.8710 (6)	0.5311 (5)
C(6)	0.4306 (7)	0.6734 (7)	0.4824 (6)
O(6)	0.4396 (6)	0.6154 (5)	0.5432 (4)
C(7)	0.6601 (10)	0.6797 (8)	0.1844 (7)
O(7)	0.7377 (7)	0.6147 (6)	0.1401 (5)
C(8)	0.6759 (9)	0.7986 (8)	0.3063 (7)
O(8)	0.7598 (7)	0.8014 (7)	0.3337 (5)
Cp(1)	0.3417 (5)	0.4466 (5)	0.1899 (3)
Cp(2)	0.2903 (5)	0.4365 (5)	0.2788 (3)
Cp(3)	0.1690 (5)	0.5066 (5)	0.2910 (4)
Cp(4)	0.1454 (5)	0.5600 (5)	0.2096 (3)
Cp(5)	0.2521 (4)	0.5229 (5)	0.1471 (4)
Me(1)	0.4640 (6)	0.3783 (7)	0.1457 (5)
Me(2)	0.3493 (7)	0.3565 (7)	0.3452 (5)
Me(3)	0.0765 (7)	0.5115 (8)	0.3719 (5)
Me(4)	0.0255 (6)	0.6353 (8)	0.1907 (5)
Me(5)	0.2638 (7)	0.5504 (7)	0.0501 (4)
Cp(6)	0.1333 (6)	0.9066 (5)	0.4068 (4)
Cp(7)	0.2069 (5)	0.9111 (5)	0.4677 (3)
Cp(8)	0.2097 (5)	0.8307 (4)	0.5316 (4)
Cp(9)	0.1378 (5)	0.7766 (5)	0.5101 (4)
Cp(10)	0.0906 (6)	0.8235 (4)	0.4330 (4)
Me(6)	0.0864 (8)	0.9904 (6)	0.3385 (5)
Me(7)	0.2626 (8)	0.9927 (6)	0.4692 (5)
Me(8)	0.2590 (8)	0.8194 (6)	0.6173 (5)
Me(9)	0.1087 (8)	0.6906 (6)	0.5637 (5)
Me(10)	−0.0074 (8)	0.8028 (6)	0.3962 (5)
Cp(11)	0.6556 (6)	0.8980 (5)	0.1255 (4)
Cp(12)	0.5882 (5)	0.9732 (5)	0.1918 (4)
Cp(13)	0.4637 (5)	0.9938 (6)	0.1912 (4)
Cp(14)	0.4541 (5)	0.9313 (5)	0.1246 (4)
Cp(15)	0.5727 (4)	0.8721 (5)	0.0840 (4)
Me(11)	0.7883 (6)	0.8603 (8)	0.0991 (6)
Me(12)	0.6384 (7)	1.0318 (8)	0.2431 (6)
Me(13)	0.3616 (6)	1.0790 (8)	0.2407 (7)
Me(14)	0.3405 (6)	0.9340 (8)	0.0974 (6)
Me(15)	0.6039 (7)	0.8062 (8)	0.0042 (6)

[a] Atomic coordinates for the disordered CH_2Cl_2 molecule were not varied.

Systematic absences of $h + k$ odd for hkl and l odd for $h0l$ indicated that the probable space groups were $Cmc2_1$, $C2cm$ (a nonstandard setting of $Ama2$), and $Cmcm$. The choice of $Cmc2_1$ was based upon the close correlation of the intensity data from a Wilson plot of the normalized structure factors with a noncentrosymmetric distribution. This selection was verified by the successful solution and refinement of the structure only under $Cmc2_1$ symmetry. Each of the four molecules lies on a mirror plane such that the crystallographically independent unit consists of one-half molecule.

Initial coordinates for the one independent Mo and three independent Co atoms were determined via the application of

---

(25) Although the hydrogen atoms are placed in idealized positions, RAELS[23] reports estimated standard deviations for these atoms. These estimates reflect the errors associated with the orientations of the local axial systems (which are calculated from the crystallographic coordinates of the ring carbon atoms) and do not reflect the actual estimated standard deviations of the fractional coordinates of the hydrogen atoms. Likewise, the thermal factors and associated estimated standard deviations reported for the hydrogen atoms do not imply that these parameters have been determined accurately for this structure. These values arise from the calculation of the librational-like thermal motion of each η^5-C_5Me_5 group which has hydrogen atoms situated at idealized positions.

(26) Rae, A. D. *Acta Crystallogr., Sect. A: Cryst. Phys., Diffr., Theor. Gen. Crystallogr.* **1975**, *A31*, 570–574.

(27) An absorption tensor is calculated from ΔF values using an option of the program RAELS.[23,28] The correction is similar to that used by Hope.[29]

(28) Rae, A. D. "The Refinability of Absorption Corrections", presented at the Annual Meeting of the American Crystallographic Association; McMaster University: Hamilton, Ontario, Canada, June 1986; Abstract PA14.

(29) Hope, H., personal communication (Feb 1984) to L. F. Dahl. The Hope program ABSORPTION (Hope, H.; Moezzi, B., unpublished results) utilizes an empirical absorption tensor from an expression relating $|F_o|$ and $|F_c|$.

(30) The unweighted and weighted discrepancy factors used are $R_1(F) = [\sum||F_o| - |F_c||/\sum|F_o|] \times 100$ and $R_2(F) = [\sum w_i||F_o| - |F_c||^2/\sum w_i|F_o|^2]^{1/2} \times 100$. All least-squares refinements were based on the minimization of $\sum w_i||F_o| - |F_c||^2$ with individual weights of $w_i = \sigma^2(F_o)$ assigned on the basis of the estimated standard deviations of the observed structure factors. Atomic scattering factors and anomalous dispersion corrections were taken from ref 31.

(31) *International Tables for X-ray Crystallography*; Kynoch: Birmingham, England, 1974; Vol. IV, pp 149, 155–158.

Table III. Selected Interatomic Distances and Bond Angles for $(\eta^5\text{-}C_5Me_5)_3Mo_3Co_2(CO)_8(\mu_3\text{-}NH)(\mu_4\text{-}N)\bullet CH_2Cl_2$

A. Interatomic Distances (Å)

Mo(1)-Mo(2)	2.978 (1)	Mo(1)-Co(1)	2.703 (1)
Mo(2)-Co(1)	2.574 (1)	Mo(2)-Co(2)	2.682 (1)
Mo(3)-Co(1)	2.792 (1)	Mo(3)-Co(2)	2.787 (1)
Co(1)-Co(2)	2.476 (2)	Mo(2)-N(1)	1.928 (7)
Mo(3)-N(1)	1.957 (7)	Co(1)-N(1)	1.940 (7)
Co(2)-N(1)	1.985 (7)	Mo(1)-N(2)	2.015 (7)
Mo(2)-N(2)	2.020 (7)	Co(1)-N(2)	2.001 (7)
Mo(1)-C(1)	1.975 (10)	Mo(1)-C(2)	1.944 (11)
Mo(2)-C(6)	2.145 (9)	Mo(3)-C(7)	1.952 (11)
Mo(3)-C(8)	1.945 (10)	Co(1)-C(1)	2.231 (9)
Co(1)-C(3)	1.782 (10)	Co(2)-C(4)	1.773 (11)
Co(2)-C(5)	1.796 (10)	Co(2)-C(6)	1.921 (9)
Co(2)-C(8)	2.466 (10)	N(1)-N(2)	2.988 (9)
C(1)-O(1)	1.175 (10)	C(2)-O(2)	1.180 (11)
C(3)-O(3)	1.136 (10)	C(4)-O(4)	1.146 (11)
C(5)-O(5)	1.129 (10)	C(6)-O(6)	1.174 (9)
C(7)-O(7)	1.186 (11)	C(8)-O(8)	1.171 (11)

B. Bond Angles (deg)

Mo(2)-Mo(1)-Co(1)	53.6 (0)	Mo(1)-Mo(2)-N(1)	90.5 (2)
Mo(1)-Mo(2)-Co(1)	57.7 (0)	Co(1)-Mo(2)-N(1)	48.5 (2)
Mo(1)-Mo(2)-Co(2)	113.7 (0)	Co(2)-Mo(2)-N(1)	47.6 (2)
Co(1)-Mo(2)-Co(2)	56.2 (0)	Co(1)-Mo(3)-N(1)	44.0 (2)
Co(1)-Mo(3)-Co(2)	52.7 (0)	Co(2)-Mo(3)-N(1)	45.4 (2)
Mo(1)-Co(1)-Mo(2)	68.7 (0)	Mo(1)-Co(1)-N(1)	98.9 (2)
Mo(1)-Co(1)-Mo(3)	125.0 (0)	Mo(2)-Co(1)-N(1)	48.1 (2)
Mo(2)-Co(1)-Mo(3)	92.5 (0)	Mo(3)-Co(1)-N(1)	44.5 (2)
Mo(1)-Co(1)-Co(2)	132.5 (1)	Co(2)-Co(1)-N(1)	51.7 (2)
Mo(3)-Co(1)-Co(2)	63.5 (0)	Mo(2)-Co(2)-N(1)	45.8 (2)
Mo(2)-Co(1)-Co(2)	64.1 (0)	Mo(3)-Co(2)-N(1)	44.6 (2)
Mo(2)-Co(2)-Mo(3)	90.4 (0)	Co(1)-Co(2)-N(1)	50.1 (2)
Mo(2)-Co(2)-Co(1)	59.7 (0)	Mo(2)-N(1)-Mo(3)	174.4 (4)
Mo(3)-Co(2)-Co(1)	63.8 (0)	Mo(2)-N(1)-Co(1)	83.4 (3)
Mo(2)-N(1)-Co(2)	86.5 (3)	Mo(1)-N(2)-Mo(2)	95.1 (3)
Mo(3)-N(1)-Co(1)	91.5 (3)	Mo(1)-N(2)-Co(1)	84.6 (3)
Mo(3)-N(1)-Co(2)	90.0 (3)	Mo(2)-N(2)-Co(1)	79.6 (2)
Co(1)-N(1)-Co(2)	78.2 (2)	Mo(1)-C(1)-O(1)	158.2 (7)
Mo(2)-Mo(1)-N(2)	42.5 (2)	Co(1)-C(1)-O(1)	121.6 (7)
Co(1)-Mo(1)-N(2)	47.5 (2)	Mo(1)-C(2)-O(2)	167.8 (9)
Mo(1)-Mo(2)-N(2)	42.4 (2)	Co(1)-C(3)-O(3)	179.0 (8)
Co(1)-Mo(2)-N(2)	49.9 (2)	Co(2)-C(4)-O(4)	172.8 (9)
Co(2)-Mo(2)-N(2)	88.7 (2)	Co(2)-C(5)-O(5)	173.7 (9)
N(1)-Mo(2)-N(2)	98.3 (3)	Mo(2)-C(6)-O(6)	139.0 (7)
Mo(1)-Co(1)-N(2)	47.9 (2)	Co(2)-C(6)-O(6)	138.2 (7)
Mo(2)-Co(1)-N(2)	50.5 (2)	Mo(3)-C(7)-O(7)	161.6 (8)
Mo(3)-Co(1)-N(2)	143.0 (2)	Mo(3)-C(8)-O(8)	163.4 (9)
Co(2)-Co(1)-N(2)	95.2 (2)	Co(2)-C(8)-O(8)	119.1 (7)
N(1)-Co(1)-N(2)	98.6 (3)		

Table IV. Crystal Data and Details of Data Collection and Refinement of $(\eta^5\text{-}C_5Me_5)_2Mo_2Co_3(CO)_{10}(\mu_5\text{-}N)\bullet C_6H_{14}$

fw	968.35
cryst system	orthorhombic
cell constants (23 °C)	
a, b, c (Å)	14.770 (2), 24.846 (10), 9.357 (2)
V (Å^3)	3987
space group	$Cmc2_1$
Z	4
d_{calcd} (g/cm^3)	1.61
radiatn (λ, Å)	Mo K$\bar{\alpha}$ (0.71073)
μ (cm^{-1})	17.11
data-collectn temp (°C)	23
scan mode	θ–2θ
2θ limits (deg)	3.0–55.0
scan speed (deg/min)	variable (2.0–24.0)
scan width (deg above Kα_1/below Kα_2	1.0/1.0
bkgd anal.	profile
std reflctns/freq	224, 113/2 per 98
cutoff obsd data	$I_o > 3\sigma(I_o)$
no. of indep obsd data	1875
no. of parameters	167
goodness-of-fit	1.57
$R_1(F)$, $R_2(F)$ (%)	3.78, 4.05

Table V. Atomic Coordinates for $(\eta^5\text{-}C_5Me_5)_2Mo_2Co_3(CO)_{10}(\mu_5\text{-}N)\bullet C_6H_{14}$[a]

atom	x	y	z
Mo(1)	0.3634 (0)	0.1464 (0)	0.2660 (1)
Co(1)	0.5000 (0)	0.1721 (1)	0.4408 (2)
Co(2)	0.5000 (0)	0.0894 (0)	0.3805 (2)
Co(3)	0.5000 (0)	0.2075 (1)	0.2044 (2)
N	0.5000 (0)	0.1436 (3)	0.2558 (7)
C(1)	0.3330 (7)	0.1698 (3)	0.4606 (8)
O(1)	0.2971 (5)	0.1820 (3)	0.5606 (7)
C(2)	0.3612 (6)	0.2169 (3)	0.2238 (8)
O(2)	0.3227 (5)	0.2519 (2)	0.2136 (7)
C(3)	0.5000 (0)	0.1832 (5)	0.6268 (9)
O(3)	0.5000 (0)	0.1895 (4)	0.7462 (8)
C(4)	0.5000 (0)	0.2363 (4)	0.3919 (9)
O(4)	0.5000 (0)	0.2734 (3)	0.4375 (7)
C(5)	0.5000 (0)	0.0372 (4)	0.2827 (9)
O(5)	0.5000 (0)	0.0013 (4)	0.2267 (9)
C(6)	0.4122 (8)	0.0812 (3)	0.5016 (8)
O(6)	0.3582 (6)	0.0709 (3)	0.5869 (8)
C(7)	0.5000 (0)	0.2563 (5)	0.0883 (11)
O(7)	0.5000 (0)	0.2865 (4)	0.0141 (9)
Hex(1)	0.0520 (0)	0.0375 (0)	−0.0812 (0)
Hex(2)	0.0477 (0)	0.1123 (0)	−0.2328 (0)
Hex(3)	0.0000 (0)	0.0425 (0)	0.0531 (0)
Hex(4)	0.0000 (0)	0.1174 (0)	−0.1246 (0)
Hex(5)	0.1046 (0)	0.0778 (0)	−0.1630 (0)
Hex(6)	0.0579 (0)	0.0762 (0)	−0.0269 (0)
Hex(7)	0.0606 (0)	−0.0606 (0)	0.2356 (0)
Cp(1)	0.2167 (4)	0.1144 (2)	0.2691 (5)
Cp(2)	0.2740 (3)	0.0822 (2)	0.2008 (5)
Cp(3)	0.3070 (4)	0.1027 (2)	0.0743 (5)
Cp(4)	0.2701 (4)	0.1477 (2)	0.0644 (5)
Cp(5)	0.2143 (4)	0.1550 (2)	0.1848 (5)
Me(1)	0.1592 (6)	0.1051 (2)	0.3976 (8)
Me(2)	0.2784 (5)	0.0306 (2)	0.2354 (7)
Me(3)	0.3646 (6)	0.0796 (3)	−0.0354 (8)
Me(4)	0.2786 (6)	0.1796 (3)	−0.0611 (8)
Me(5)	0.1528 (5)	0.1956 (2)	0.2076 (7)

[a] Atomic coordinates for the disordered hexane molecule were not varied.

MULTAN.[32] The remaining non-hydrogen atoms were located from a combination of successive difference maps coupled with several cycles of isotropic least-squares refinement with RAELS.[23] At this stage, the independent pentamethylcyclopentadienyl ligand with hydrogen atoms included at idealized positions was introduced into the refinement as a rigid group with local C_{5v} symmetry. Both the positional and thermal parameters of the $(\eta^5\text{-}C_5Me_5)$ group were refined by use of a subsidiary axial system.[24,25] With the exception of the carbon atoms belonging to a highly disordered hexane molecule of crystallization (for which isotropic thermal factors were used) and the $(\eta^5\text{-}C_5Me_5)$ ring, all other non-hydrogen atoms were refined with individual anisotropic thermal parameters. The thermal librational-like motion of the $(\eta^5\text{-}C_5Me_5)$ ring was treated with a TLX model.[25,26] During a later stage of the refinement, the methyl substituents of the pentamethylcyclopentadienyl ligand were individually allowed to move away from the plane containing the ring carbon atoms. An empirical absorption correction was applied to the intensity data.[27-29]

The full least-squares refinement converged at $R_1(F) = 3.78\%$ and $R_2(F) = 4.05\%$ with a data-to-parameter ratio of 11.2/1.[30] In the final cycle, a relatively large parameter change-to-esd ratio (2.38) was observed for the isotropic thermal parameter of one of the solvent carbon atoms. All other parameter change-to-estimated standard deviation ratios were 0.3 or less. A test of the handedness of the noncentrosymmetric structure was performed by a similar refinement carried out with the signs of all atomic coordinates reversed. This resulted in an increase of $R_1(F)$ from 3.78% to 3.94% with no significant changes in the measured bond lengths; thus the handedness of the original refinement was as-

---

(32) (a) Main, P.; Lessinger, L.; Woolfson, M. M.; Germain, G.; Declercq, J.-P. MULTAN-78. (b) Germain, G.; Main, P.; Woolfson, M. M. *Acta Crystallogr., Sect. A: Cryst. Phys., Diffr., Theor. Gen. Crystallogr.* **1971**, *A27*, 368–376.

Table VI. Selected Interatomic Distances and Bond Angles for $(\eta^5\text{-}C_5Me_5)_2Mo_2Co_3(CO)_{10}(\mu_5\text{-}N)\bullet C_6H_{14}$

A. Interatomic Distances (Å)

Mo(1)–Co(1)	2.701 (1)	Mo(1)–Co(2)	2.815 (1)
Mo(1)–Co(3)	2.740 (1)	Co(1)–Co(2)	2.453 (2)
Co(1)–Co(3)	2.437 (2)	Mo(1)–N	2.021 (1)
Co(1)–N	1.917 (12)	Co(2)–N	1.951 (10)
Co(3)–N	1.905 (8)	Mo(1)–C(1)	1.994 (11)
Mo(1)–C(2)	2.070 (9)	Co(1)–C(1)	2.474 (10)
Co(1)–C(3)	1.769 (13)	Co(1)–C(4)	1.907 (12)
Co(2)–C(5)	1.761 (13)	Co(2)–C(6)	1.738 (12)
Co(3)–C(2)	2.075 (9)	Co(3)–C(4)	1.941 (15)
Co(3)–C(7)	1.777 (15)	C(1)–O(1)	1.131 (11)
C(2)–O(2)	1.164 (9)	C(3)–O(3)	1.132 (15)
C(4)–O(4)	1.151 (14)	C(5)–O(5)	1.161 (15)
C(6)–O(6)	1.168 (12)	C(7)–O(7)	1.116 (16)

B. Bond Angles (deg)

Co(1)–Mo(1)–Co(2)	52.8 (0)	Mo(1)–N–Co(1)	86.6 (3)
Co(1)–Mo(1)–Co(3)	53.2 (0)	Mo(1)–N–Co(2)	90.2 (3)
Co(2)–Mo(1)–Co(3)	85.9 (0)	Mo(1)–N–Co(3)	88.5 (2)
Mo(1)–Co(1)–Co(2)	66.0 (0)	Co(1)–N–Co(2)	78.7 (5)
Mo(1)–Co(1)–Co(3)	64.2 (0)	Co(1)–N–Co(3)	79.2 (3)
Co(2)–Co(1)–Co(3)	101.4 (1)	Co(2)–N–Co(3)	157.9 (7)
Mo(1)–Co(2)–Co(1)	61.3 (0)	Mo(1)–C(1)–O(1)	165.0 (9)
Mo(1)–Co(3)–Co(1)	62.6 (0)	Co(1)–C(1)–O(1)	121.4 (8)
Co(1)–Mo(1)–N	45.1 (3)	Mo(1)–C(2)–O(2)	151.1 (8)
Co(2)–Mo(1)–N	43.9 (3)	Co(3)–C(2)–O(2)	126.1 (7)
Co(3)–Mo(1)–N	44.0 (2)	Co(1)–C(3)–O(3)	178.8 (14)
Mo(1)–Co(1)–N	48.3 (0)	Co(1)–C(4)–O(4)	144.3 (12)
Co(2)–Co(1)–N	51.3 (3)	Co(3)–C(4)–O(4)	137.1 (11)
Co(3)–Co(1)–N	50.2 (3)	Co(2)–C(5)–O(5)	175.6 (17)
Mo(1)–Co(2)–N	45.9 (0)	Co(2)–C(6)–O(6)	172.2 (9)
Co(1)–Co(2)–N	50.0 (3)	Co(3)–C(7)–O(7)	179.2 (16)
Mo(1)–Co(3)–N	47.5 (0)		
Co(1)–Co(3)–N	50.6 (4)		

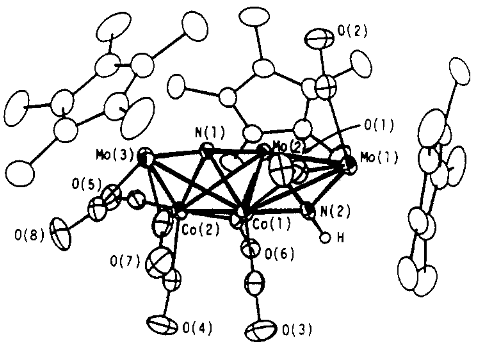

Figure 1. Molecular geometry of $(\eta^5\text{-}C_5Me_5)_3Mo_3Co_2(CO)_8(\mu_3\text{-}NH)(\mu_4\text{-}N)$. The imido hydrogen atom, which was not located directly from the X-ray structural refinement, is shown in its idealized location; its formulation was clearly established from characteristic ^{15}N NMR and solid-state IR spectra.

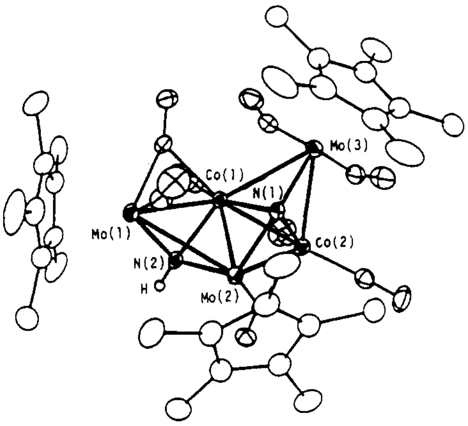

Figure 2. Another view of the molecular geometry of $(\eta^5\text{-}C_5Me_5)_3Mo_3Co_2(CO)_8(\mu_3\text{-}NH)(\mu_4\text{-}N)$.

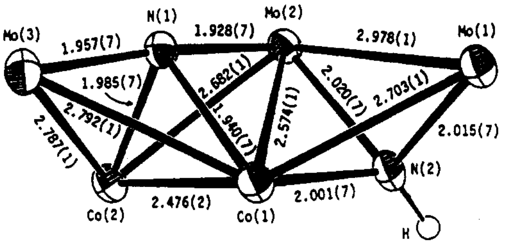

Figure 3. Architecture of the $Mo_3Co_2(\mu_3\text{-}NH)(\mu_4\text{-}N)$ core of $(\eta^5\text{-}C_5Me_5)_3Mo_3Co_2(CO)_8(\mu_3\text{-}NH)(\mu_4\text{-}N)$. The butterfly $Mo_2Co_2(\mu_4\text{-}N)$ moiety, linked to a five-electron-donating $Mo(\eta^5\text{-}C_5Me_5)(CO)_2(\mu_3\text{-}NH)$ fragment, corresponds to a 62-electron system in which the μ_4-N ligand donates five electrons.

sumed to be correct. A final difference map revealed no abnormal features; the largest residual densities corresponded to several small peaks (of electron densities less than 10% of that of a typical carbon atom) located at nonmeaningful atomic sites near the molybdenum atoms.

Positional parameters for the non-hydrogen atoms from the last full-matrix least-squares cycle are given in Table V. Interatomic distances and bond angles for **2·hex** are given in Table VI. Thermal parameters for all non-hydrogen atoms, coordinates and temperature factors for all hydrogen atoms, and a listing of observed and calculated structure factor amplitudes are available as supplementary material.

Results and Discussion

Structural Analysis of $(\eta^5\text{-}C_5Me_5)_3Mo_3Co_2(CO)_8(\mu_3\text{-}NH)(\mu_4\text{-}N)$ (1). (a) Geometry and Composition of the Cluster Core. The unique geometry of 1 (Figures 1–3) can be described as being based on a Mo_2Co_2 butterfly fragment with an additional Mo atom bridging one of the Mo(wingtip)–Co(backbone) bonds. The butterfly moiety of 1 is defined by Mo(2), Mo(3), Co(1), and Co(2) with both of the Co atoms occupying backbone (hinge) positions. The Co(1)–Mo(2) edge is spanned by Mo(1) to give an edge-fused Mo_2Co triangle. The core of 1 is completed by a nitrido atom which is contained within the Mo_2Co_2 butterfly moiety and by an imido (NH) ligand which caps the Mo_2Co triangular face.

On the basis of the previous synthesis and structural characterization of a 62-electron $[Fe_4(CO)_{12}(\mu_4\text{-}N)]^-$ monoanion with a butterfly iron nitride core from a precursor which contained a bound nitrosyl ligand,[33] the identity of the butterfly-bound light atom in 1 was initially assumed to be nitrogen. When the X-ray crystallographic refinement of $1\cdot CH_2Cl_2$ was performed with the scattering factor of the butterfly-bridging light atom assigned as a nitrogen, the isotropic thermal parameter of that atom was found to be similar to those of the metal atoms to which it is bound. Changing the scattering factor of the buterfly-bridging light atom to that of a carbon atom resulted in its isotropic thermal parameter becoming nonpositive definite (i.e., a negative value) due to insufficient electron density at that atom. When the scattering factor of an oxygen atom was used, the isotropic thermal parameter became unreasonably large. These results for the well-behaved refinement of $1\cdot CH_2Cl_2$ provide strong crystallographic evidence that the butterfly-bound atom is a nitride ligand. This conclusion, which is consistent with the elemental analysis of 1, was substantiated from the spectroscopic data (vide infra).

Since Mo-containing triangular metal clusters are often found to be capped by oxygen atoms, the light atom cap-

---

(33) Fjare, D. E.; Gladfelter, W. L. *Inorg. Chem.* **1981**, *20*, 3533–3539.

ping the Mo_2Co triangle was initially assumed to be oxygen. When the initial refinement was conducted with the scattering factor of the capping atom assigned as oxygen, its isotropic thermal parameter became (unrealistically) much larger than those of the metals to which it is bound. A similar refinement conducted with the scattering factor of a carbon atom resulted in a nonpositive definite thermal parameter (i.e., a negative value) for the capping atom. The isotropic thermal parameter of the capping atom became similar to those of the coordinated cobalt and Mo atoms only when the scattering factor of a nitrogen atom was used. Thus, crystallographic evidence strongly indicates that the trigonal-pyramidal capping atom is nitrogen. This assignment, which is in accordance with the elemental analysis of $1 \cdot CH_2Cl_2$, was substantiated by the spectroscopic data. Because organometallic clusters possessing a "bare" *trigonal-pyramidal* μ_3-N ligand have not as yet been isolated, we then assumed the capping ligand to be a four-electron-donating imido (μ_3-NH) ligand. Although a residual peak which could be unambiguously assigned to the imido hydrogen atom was not located from a final difference Fourier map, the existence of the hydrogen atom was subsequently verified by both ^{15}N NMR and infrared spectroscopy (vide infra).

(b) Metal-Metal Bonding in $(\eta^5\text{-}C_5Me_5)_3Mo_3Co_2(CO)_8(\mu_3\text{-}NH)(\mu_4\text{-}N)$ (1). The metal core of 1 can be described as being composed of three metal triangles fused at two edges. The Mingos fusion rule[34] predicts a valence electron count of 3(48) − 2(34) = 76 electrons, as observed. Furthermore, this electron count is in agreement with the Lauher model[35] which for the five metal atoms with seven bonding edges predicts 5(18) − 7(2) = 76 electrons. The Lauher model is based upon an electron-precise system that can be described from a valence-bond representation in terms of an electron-pair bond along each metal–metal edge. Application of the fusion rule[34] also indicates electron-pair metal–metal bonds because the fragments (viz., saturated metal triangles and dimers) are electron precise.

Alternatively, 1 can be considered to be an electron-precise derivative of a butterfly Mo_2Co_2 cluster; the butterfly portion of 1 consists of the 57-electron $(\eta^5\text{-}C_5Me_5)_2Mo_2Co_2(CO)_6(\mu_4\text{-}N)$ fragment which is coordinated by additional electron-pair bonds from the Mo and Co atoms of one bonding Co–Mo edge to both the Mo and N atoms of a five-electron-donating $Mo(\eta^5\text{-}C_5Me_5)(CO)_2(\mu_3\text{-}NH)$ moiety. The Mo(1) atom also attains a closed-shell electronic configuration. This Mo(2)–Co(1) edge-fusion of the resulting "closed" tetrahedral $Mo_2Co(\mu_3\text{-}NH)$ system to the central $Mo_2Co_2(\mu_4\text{-}N)$ core gives rise to a 62-electron count for the butterfly portion of 1. This electronic configuration is in agreement with electron-counting rules which normally require 62 electrons for a butterfly metal cluster. Application of the Mingos fusion rule[34] to a butterfly metal cluster edge-fused to a metal triangle predicts (62 + 48 − 34) = 76 electrons. The self-consistency of these qualitative bonding models in indicating that each metal–metal contact in 1 can be formulated from a valence-bond viewpoint as a localized electron-pair bond points to Co(1) utilizing *four* valence skeletal orbitals in its bonding interactions with Co(2), Mo(1), Mo(2), and Mo(3) (in contrast to three such orbitals being used by each of the other four metal atoms).

In accordance with these electronic considerations based on localized electron-pair metal–metal bonds, definitive evidence for the anticipated diamagnetism of 1 is given by the observance in a room-temperature proton NMR spectrum of 1 in $CDCl_3$ of very sharp resonances within the normal range for three nonequivalent $(\eta^5\text{-}C_5Me_5)$ ligands. Further support for a localized bonding description is given by the metal–metal bond lengths in 1 being similar to metal–metal single-bond lengths found in other organometallic compounds. The bond length of 2.978 (1) Å for the Mo(1)–Mo(2) edge is within the range of 2.9–3.0 Å found[5,36] for single bonds between Mo atoms which are in a formal oxidation state of +2. The bond lengths of 2.792 (1) and 2.787 (1) Å determined for the non-carbonyl-bridged Mo(3)–Co(1) and Mo(3)–Co(2) edges are expectedly longer than the bond lengths of 2.703 (1) and 2.682 (1) Å determined for the carbonyl-bridged Mo(1)–Co(1) and Mo(2)–Co(2) edges. These Mo–Co bond lengths are similar to the Mo–Co bonds in other low-valent Mo–Co clusters including $(\eta^5\text{-}C_5H_5)MoCo_3(CO)_{11}$ (2.752 (4), 2.728 (4), and 2.741 (3) Å),[37] $(\eta^5\text{-}C_5Me_5)_2Mo_2Co(\eta^5\text{-}C_5H_5)(CO)_4(\mu_3\text{-}O)$ (2.716 (2) and 2.618 (2) Å),[4,6a] $(\eta^5\text{-}C_5Me_5)_3Mo_3Co(CO)_5(\mu_2\text{-}O)(\mu_3\text{-}O)$ (2.684 (2), 2.627 (2), and 2.638 (2) Å),[4,6a] and 2 (2.701 (1) and 2.805 (1) Å). The considerably shorter Mo(2)–Co(1) bond length of 2.574 (1) Å in 1 is presumably due to this Mo–Co edge being spanned by both a nitrido and an imido ligand. The Co(1)–Co(2) bond length of 2.476 (2) Å is typical of values observed for Co–Co single bonds in a variety of compounds including those in $(\eta^5\text{-}C_5H_5)MoCo_3(CO)_{11}$ (2.473 (7), 2.512 (6), and 2.467 (6) Å)[37] and in 2 (2.453 (2) and 2.437 (2) Å).

The trigonal-pyramidal NH ligand in 1 is equidistant from the cobalt and two molybdenum atoms. The Co(1)–N(2) bond length of 2.001 (7) Å is experimentally equivalent to the Mo(1)–N(2) and Mo(2)–N(2) bond lengths of 2.015 (7) and 2.020 (7) Å, respectively, but significantly longer than the Co–NH bond lengths in the 48-electron triangular metal imido clusters $FeCo_2(CO)_9(\mu_3\text{-}NH)$ (1.859 Å (average))[38] and the $[Co_3(\eta^5\text{-}C_5H_4Me)_3(\mu_3\text{-}NO)(\mu_3\text{-}NH)]^+$ monocation (1.835 Å (average)).[8f]

The geometries of a large number of 62-electron butterfly metal clusters containing μ_4-N or μ_4-C atoms have been determined by X-ray diffraction studies.[39–44] Gladfelter[39] pointed out that in each of the structurally characterized butterfly metal nitride clusters the metal–nitrogen distances are much shorter to the wingtip metal atoms than to the backbone metal atoms. This bond-length difference was attributed to enhanced metal–nitrogen π-bonding interactions along the exposed edge. Indeed, this bond-length variation can be seen in butterfly metal clusters containing an exposed carbide ligand as well as those containing an exposed nitride.[44] Theoretical

---

[34] (a) Mingos, D. M. P. *J. Chem. Soc., Chem. Commun.* **1983**, 706–708. (b) Mingos, D. M. P. *Acc. Chem. Res.* **1984**, *17*, 311–319.

[35] Lauher, J. W. *J. Am. Chem. Soc.* **1978**, *100*, 5305–5315.

[36] Since each Mo atom in 1 is bonded to a $C_5Me_5^-$ ligand in addition to the nitrido (N^{3-}) and/or the imido (NH^{2-}) ligand whereas one Co atom is bonded only to the nitrido ligand and the other Co atom only to the nitrido and imido ligands, we assign a formal oxidation state of +1 to each Co atom and +2 to each Mo atom. Single bonds between high-valent Mo atoms tend to be much shorter.[5]

[37] Schmid, G.; Bartl, K.; Boese, R. *Z. Naturforsch., B: Anorg. Chem., Org. Chem.* **1977**, *32B*, 1277–1283.

[38] Fjare, D. E.; Keyes, D. G.; Gladfelter, W. L. *J. Organomet. Chem.* **1983**, *250*, 383–394.

[39] Gladfelter, W. L. *Adv. Organomet. Chem.* **1985**, *24*, 41–86.

[40] Bradley, J. S. *Adv. Organomet. Chem.* **1983**, *22*, 1–58.

[41] (a) Muetterties, E. L.; Stein, J. *Chem. Rev.* **1979**, *79*, 479–490. (b) Tachikawa, M.; Muetterties, E. L. *Prog. Inorg. Chem.* **1981**, *28*, 203–238.

[42] (a) Holt, E. M.; Whitmire, K. H.; Shriver, D. F. *J. Am. Chem. Soc.* **1982**, *104*, 5621–5626. (b) Kolis, J. W.; Basolo, F.; Shriver, D. F. *J. Am. Chem. Soc.* **1982**, *104*, 5626–5630. (c) Drezdzon, M. A.; Whitmire, K. H.; Bhattacharyya, A. A.; Hsu, W.-L.; Nagel, C. C.; Shore, S. G.; Shriver, D. F. *J. Am. Chem. Soc.* **1982**, *104*, 5630–5633.

[43] Gladfelter, W. L. In *Organometallic Compounds: Synthesis, Structure, and Reactivity*; Shapiro, B. L.; Ed.; Texas A&M University: College Station, TX, 1983.

calculations on several butterfly metal carbide clusters have shown that this effect is, as postulated, due to both strong π-bonding and σ-bonding interactions between the wingtip metal atoms and the carbide ligand.[45,46]

Compound 1 differs from all previously characterized butterfly metal nitride clusters in that all of the metal-to-nitride distances in the butterfly portion of 1 are virtually identical (M–N = 1.95 Å (average)). The equivalent metal-to-nitride distances in 1 can be readily rationalized in terms of the greater covalent radius of Mo versus that of Co; the radius of Mo is estimated to be ca. 0.17 Å larger than that of Co in 1, as indicated by the difference between the Mo–CO(terminal) and Co–CO(terminal) bond lengths (1.95 Å (average) versus 1.78 Å (average)). For a typical butterfly metal nitride cluster, such as the [Fe$_4$(CO)$_{12}$(μ_4-N)]$^-$ monoanion,[44a] the metal(wingtip)-to-nitride bond lengths are 0.13 Å shorter than the metal(backbone)-to-nitride bond lengths. Hence, the 0.17 Å greater covalent radii of the wingtip Mo atoms in 1 apparently compensate for the intrinsically shorter metal(wingtip)-to-nitride bonds due primarily to enhanced π-bonding interactions along the exposed metal(wingtip)–nitride–metal(wingtip) edge.

Structural Analysis and Resulting Bonding Implications of (η^5-C$_5$Me$_5$)$_2$Mo$_2$Co$_3$(CO)$_{10}$(μ_5-N)·C$_6$H$_{14}$ (2·hex). The crystal structure of 2 was found to be composed of discrete molecules whose geometry consists of a square-pyramidal array of two Mo and three Co atoms with a nitrido atom located slightly below the basal plane of two Co and two Mo atoms. The identity of this pentametal-coordinated atom as a nitrogen was clearly established from the crystallographic analysis. Refinements conducted with the scattering factor of this atom assigned as a carbon, a nitrogen, or an oxygen atom were carried out. When assigned as a carbon, the isotropic thermal parameter of this atom became nonpositive definite due to insufficient electron density at that site. When designated as an oxygen, the refinement resulted in an atomic isotropic thermal parameter that was (unrealistically) much larger than the thermal motion of the metal atoms to which it is bound. When denoted as a nitrogen, the resulting thermal motion of this atom became nearly identical with the thermal motions of the metal atoms to which it is bound. This convincing evidence that 2 contains a nitride atom results in the valence electron count of this square-pyramidal metal cluster being the same as those in the other known square-pyramidal metal clusters (vide infra).

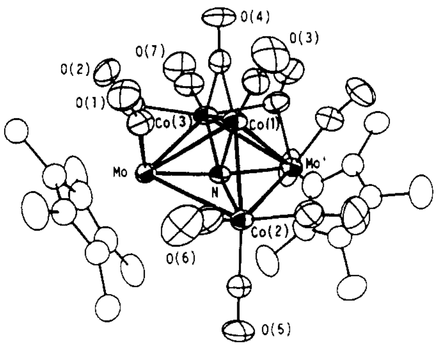

Figure 4. Molecular geometry of (η^5-C$_5$Me$_5$)$_2$Mo$_2$Co$_3$(CO)$_{10}$(μ_5-N), a 74-electron square-pyramidal mixed-metal cluster that contains a pentametal-coordinated nitride atom. This molecule contains a crystallographically imposed mirror plane which passes through the three cobalt atoms, the nitride atom, and one bridging and three terminal carbonyl groups.

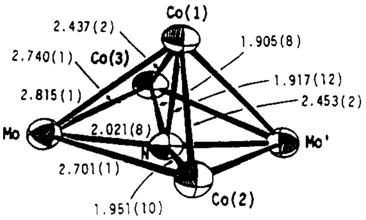

Figure 5. Architecture of the Mo$_2$Co$_3$(μ_5-N) core of the 74-electron (η^5-C$_5$Me$_5$)$_2$Mo$_2$Co$_3$(CO)$_{10}$(μ_5-N).

The molecular configuration of 2 is displayed in Figure 4. the architecture of the Mo$_2$Co$_3$(μ_5-N) core (Figure 5) approximately conforms to C_{2v} symmetry with a cobalt atom positioned at the apex of a square pyramid, two cobalt atoms occupying opposite corners of the base of the pyramid, and the two molybdenum atoms located in the other two basal positions. A nitride ligand, which is slightly below the base of the pyramid, is bonded to all five metal atoms. Inclusion of the two Mo-coordinated C$_5$Me$_5$ ligands and ten carbonyl groups (three of which are bridging) lowers the symmetry to the crystallographically imposed mirror plane which contains the three cobalt atoms, the nitride atom, and one bridging and three terminal carbonyl groups. The completely bonding square-pyramidal metal geometry of 2, which is characteristic of 74-electron clusters, has been shown from X-ray crystallographic studies to be also adopted by a number of other *electronically equivalent* pentametal nitrido and carbido clusters[39–42,47]

---

(44) (a) [Fe$_4$(CO)$_{12}$(μ_4-N)]$^-$ ([PPN]$^+$ salt): Fjare, D. E.; Gladfelter, W. L. *Inorg. Chem.* **1981**, *20*, 3533–3539. (b) Fe$_4$(CO)$_{12}$(μ_2-H)(μ_4-N): Tachikawa, M.; Stein, J.; Muetterties, E. L.; Teller, R. G.; Beno, M. A.; Gebert, E.; Williams, J. M. *J. Am. Chem. Soc.* **1980**, *102*, 6648–6649. (c) Fe$_4$(CO)$_{10}$(NO)(P(OMe)$_3$)(μ_4-N): Furuya, F. R.; Fjare, D. E.; Gladfelter, W. L., unpublished observations. Cited in ref 89 of a paper by Gladfelter.[39] (d) [FeRu$_3$(CO)$_{12}$(μ_4-N)]$^-$ ([NEt$_4$]$^+$ salt): Fjare, D. E.; Gladfelter, W. C. *J. Am. Chem. Soc.* **1984**, *106*, 4799–4810. (e) [FeRu$_3$(CO)$_{10}$(P(OMe)$_3$)$_2$(μ_4-N)]$^-$ ([NEt$_4$]$^+$ salt): Blohm, M. L.; Fjare, D. E.; Gladfelter, W. C. *J. Am. Chem. Soc.* **1986**, *108*, 2301–2309. (f) Ru$_4$(CO)$_{11}$(μ_2-H)$_3$(μ_4-N) and [Os$_4$(CO)$_{12}$(μ_4-N)]$^-$ ([PPN]$^+$ salt): Collins, M. A.; Johnson, B. F. G.; Lewis, J.; Mace, J. M.; Morris, J.; McPartlin, M.; Nelson, W. J. H.; Puga, J.; Raithby, P. R. *J. Chem. Soc., Chem. Commun.* **1983**, 689–691. (g) Ru$_4$(CO)$_{11}$(P(OMe)$_3$)(μ_2-H)(μ_4-N): Braga, D.; Johnson, B. F. G.; Lewis, J.; Mace, J. M.; McPartlin, M.; Puga, J.; Nelson, W. J. H.; Raithby, P. R.; Whitmire, K. H. *J. Chem. Soc., Chem. Commun.* **1982**, 1081–1983. (h) Fe$_4$(CO)$_{13}$(μ_4-C): Bradley, J. S.; Ansell, G. B.; Leonowicz, M. E.; Hill, E. W. *J. Am. Chem. Soc.* **1981**, *103*, 4968–4970. (i) [Fe$_4$(CO)$_{12}$(μ_4-C)]$^{2-}$ ([Zn(NH$_3$)$_4$]$^{2+}$ salt): Davis, J. H.; Beno, M. A.; Williams, J. M.; Zimmie, J.; Tachikawa, M.; Muetterties, e. L. *Proc. Natl. Acad. Sci. U.S.A.* **1981**, *78*, 668–671. (j) [Fe$_4$(CO)$_{12}$(μ_4-C)]$^{2-}$ ([NBzMe$_3$]$^+$ salt): Boehme, R. F.; Coppens, P. *Acta Crystallogr., Sect. B: Struct. Crystallogr. Cryst. Chem.* **1981**, *B37*, 1914–1916; (k) [Fe$_4$(CO)$_{12}$(μ_4-H)(μ_4-C)]$^-$ ([PPN]$^+$ salt): Holt, W. M.; Whitmire, K. H.; Shriver, D. F. *J. Organomet. Chem.* **1981**, *213*, 125–137.

(45) Wijeyesekera, S. D.; Hoffmann, R.; Wilker, C. N. *Organometallics* **1984**, *3*, 962–970.

(46) Harris, S.; Bradley, J. S. *Organometallics* **1984**, *3*, 1086–1093.

(47) (a) Fe$_5$(CO)$_{15}$(μ_5-C): Braye, E. H.; Dahl, L. F.; Hübel, W.; Wampler, D. L. *J. Am. Chem. Soc.* **1962**, *84*, 4633–4639. (b) Fe$_5$(CO)$_{14}$(μ_2-H)(μ_5-N): Tachakawa, M.; Stein, J.; Muetterties, E. L.; Teller, R. G.; Beno, M. A.; Gebert, E.; Williams, J. M. *J. Am. Chem. Soc.* **1980**, *102*, 6648–6649. (c) [Fe$_5$(CO)$_{14}$(μ_5-N)]$^-$ ([PPN]$^+$ salt): Gourdon, A.; Jeannin, Y. *C. R. Seances Acad. Sci.* **1982**, *295*, 1101–1104. (d) [Ru$_5$(CO)$_{14}$(μ_5-N)]$^-$ ([NBzEt$_3$]$^+$ salt): Blohm, M. L.; Gladfelter, W. L. *Organometallics* **1985**, *4*, 45–52. Blohm, M. L.; Fjare, D. E.; Gladfelter, W. L. *Inorg. Chem.* **1983**, *22*, 1004–1006. (e) [Fe$_5$(CO)$_{14}$(μ_5-C)]$^{2-}$ ([NBu$_4$]$^+$ salt): Gourdon, A.; Jeannin, Y. *C. R. Seances Acad. Sci. Paris* **1982**, *295*, 1101–1104. (f) [RhFe$_4$(CO)$_{14}$(μ_5-C)]$^-$ ([NEt$_4$]$^+$ salt): Tachikawa, M.; Sievert, A. C.; Muetterties, E. L.; Thompson, M. R.; Day, C. S.; Day, V. W. *J. Am. Chem. Soc.* **1980**, *102*, 1725–1727. (g) Ru$_5$(CO)$_{15}$(μ_5-C), Ru$_5$(CO)$_{14}$(PPh$_3$)(μ_5-C), Ru$_5$(CO)$_{13}$(PPh$_3$)$_2$(μ_5-C), and Ru$_5$(CO)$_{12}$(Ph$_2$P(CH$_2$)$_2$PPh$_2$)(μ_2-H)$_2$(μ_5-C): Johnson, B. F. G.; Lewis, J.; Nicholls, J. N.; Puga, J.; Raithby, P. R.; Rosales, M. J.; McPartlin, M.; Clegg, W. *J. Chem. Soc., Dalton Trans.* **1983**, 277–290. (h) Ru$_5$(CO)$_{13}$(Ph$_2$P(CH$_2$)$_4$PPh$_2$)(μ_5-C): Evans, J.; Gracey, B. P.; Gray, L. R.; Webster, M. *J. Organomet. Chem.* **1982**, *240*, C61–C64. (i) Os$_5$(CO)$_{15}$(μ_5-C): Jackson, P. F.; Johnson, B. F. G.; Lewis, J.; Nicholls, J. N.; McPartlin, M.; Nelson, W. J. H. *J. Chem. Soc., Chem. Commun.* **1980**, 564–566. (j) [Os$_5$(CO)$_{14}$(μ_5-C)]$^{2-}$ ([PPN]$^+$ salt) and Os$_5$(CO)$_{14}$(μ_2-AuPPh$_3$)$_2$(μ_5-C): Johnson, B. F. G.; Lewis, J.; Nelson, W. J. H.; Nicholls, J. N.; Puga, J.; Raithby, P. R.; Rosales, M. J.; Schröder, M.; Vargas, M. D. *J. Chem. Soc., Dalton Trans.* **1983**, 2447–2457.

including the prototype $Fe_5(CO)_{15}(\mu_5\text{-}C)$,[47a] $Fe_5(CO)_{14}(\mu_2\text{-}H)(\mu_5\text{-}N)$,[47b] the $[Fe_5(CO)_{14}(\mu_5\text{-}N)]^-$ monoanion,[47c] and the $[Ru_5(CO)_{14}(\mu_5\text{-}N)]^-$ monoanion.[47d] MO calculations have been performed[45] on $Fe_5(CO)_{15}(\mu_5\text{-}C)$.

The three independent Mo–Co distances in **2** range from 2.701 (1) Å to 2.815 (1) Å; these values are within the range observed for Mo–Co single bonds.[4,6b,37] The two independent Co–Co distances of 2.453 (2) and 2.437 (2) Å are also within the range observed for Co–Co single bonds.

The pentametal-coordinated nitride ligand in **2** lies 0.25 Å below the mean plane of the four basal metal atoms. The basal Co–N bond lengths of 1.951 (8) Å and 1.905 (10) Å for Co(2) and Co(3), respectively, are 0.07–0.12 Å shorter than the independent basal Mo–N bond of 2.021 (1) Å. Since each Mo is estimated to have a 0.2 Å greater covalent radius than that of cobalt (i.e., based upon the observed variation between the mean Mo–CO(terminal) and mean Co–CO(terminal) distances of 0.17 Å in **1** and 0.23 Å in **2**), the smaller than expected bond-length difference of 0.1 Å between the basal Mo–N and basal Co–N bonds in **2** may be ascribed to much stronger π-bonding interactions to the Mo atoms from the electron-donating nitride atom. The apical Co–N bond of 1.917 (12) Å in **2** is virtually identical with the basal Co–N lengths. This experimental bond-length equivalence is in sharp contrast to the previously characterized 74-electron square-pyramidal metal nitride and carbide clusters which have been found to have apical metal-to-nitrogen/carbon distances that are significantly longer by 0.1–0.4 Å than basal metal-to-nitrogen/carbon bonds.[39-42,47] This equivalence of the apical and basal Co–N distances in **2** may be ascribed to smaller than usual π-bonding nitride donation to the basal cobalt atoms due to preferential π-bonding nitride donation to the basal molybdenum atoms.

Synthesis of $(\eta^5\text{-}C_5Me_5)_3Mo_3Co_2(CO)_8(\mu_3\text{-}NH)(\mu_4\text{-}N)$ (1) and $(\eta^5\text{-}C_5Me_5)_2Mo_2Co_3(CO)_{10}(\mu_5\text{-}N)$ (2). Our study of the photolytic reaction of $Co(CO)_3NO$ (**4**) with the Mo–Mo triple-bonded dimer (**3**) was initiated in an attempt to develop a rational synthetic pathway to mixed-metal clusters which have a triply bridging nitrosyl ligand. In previous studies, we have shown that the addition of coordinatively unsaturated organometallic species to **3** can give new mixed-metal clusters.[4-7] Since **3** and its nonmethylated analogue, $Mo_2(\eta^5\text{-}C_5H_5)_2(CO)_4$, have been shown to react with both electrophilic and nucleophilic reagents,[48-51] our initial expectation was that the photolytic reaction of **3** with **4** would result in the isolation of either the unknown tetrametallic product (**5**) and/or the unknown trimetallic product (**6**). Contrary to these expectations, the reaction is a rather complicated process which gives a number of products. Examination of the solution infrared spectra that were taken periodically throughout the course of the reaction indicated that the main product of the reaction is $Mo(\eta^5\text{-}C_5Me_5)(CO)_2NO$ (**7**) and that large quantities of **7** are formed very early in the reaction with a concomitant decrease in the concentration of **4**. We have also observed the formation of **7** in both thermal and photochemical reactions of **3** with various neutral or anionic metal nitrosyl compounds.[52] While it is tempting to speculate that the formation of **7** could involve an intermediate appearance of the anticipated mixed-metal product **5** or **6**, it is quite likely that the formation of **7** occurs via some unrelated reaction, possibly the reaction of **3** with free NO.[50] Another species that appears early in the reaction, but not in large quantities, is the Mo–Mo single-bonded $Mo_2(\eta^5\text{-}C_5Me_5)_2(CO)_6$ (**8**) which is presumably formed via the reaction of **3** with free CO.[53]

The photolytic reaction of **3** and **4** in THF also produced (in addition to **7** and **8**) two new mixed-metal clusters. Separation of these products via chromatographic techniques was complicated by their similar solubilities. As a result, only minute quantities of the square-pyramidal metal cluster (**2**) were isolated, and its characterization was based primarily on the X-ray structural analysis. On the other hand, a separation scheme was developed which allowed the major mixed-metal species (**1**) to be isolated in pure form. Cluster **1**, which was characterized by elemental, spectroscopic, and X-ray diffraction analyses, was isolated in overall yields of up to 11% via column chromatography followed by recrystallization.

Spectroscopic Characterization of $(\eta^5\text{-}C_5Me_5)_3Mo_3Co_2(CO)_8(\mu_3\text{-}NH)(\mu_4\text{-}N)$ (1). Compound **1** is a highly unusual mixed-metal cluster which contains both a tetrametal-coordinated nitride ligand and a trimetal-coordinated imido ligand. A proton NMR spectrum of **1** ($CDCl_3$) displays three equivalent resonances located at δ 1.83, 1.88, and 1.95 which are assigned to the three nonequivalent $\eta^5\text{-}C_5Me_5$ ligands; no ^1H NMR resonance which could be assigned to the imido hydrogen was observed, presumably due to the broadening of the signal via coupling to the quadrupolar nitrogen atom. A $^{15}N\{H\}$ spectrum of **1** ($CDCl_3/CH_3NO_2$ at −70 °C) exhibited two signals of equal intensity located at δ 518 and 190. When the proton decoupling was removed, the signal at δ 190 was observed as a doublet ($J(^1H\text{-}^{15}N) = 76$ Hz). The resonance located at δ 518 is assigned to the butterfly-bridging nitride atom and is in agreement with the observation that butterfly-bridging nitride atoms have ^{15}N chemical shifts which range from δ 514 to 618.[39,44b,g] The ^{15}N resonance located at δ 190 was assigned to the face-capping imido ligand; two other reports of ^{15}N spectra of metal clusters containing triply or quadruply bridging imido ligands have recently appeared.[44e,54] The existence of the μ_3-NH imido ligand was further substantiated by the observation in a solid-state (KBr pellet) spectrum of **1** of a small but sharp band at 3279 cm^{-1} due to the N–H stretching frequency.

The origin of the imido hydrogen atom is unclear, with possible sources including abstraction of hydrogen from solvent and/or adventitious water which may be present in small amounts as a consequence of the aqueous preparation of **4**.[20] Recent attempts in our laboratories to synthesize triangular metal clusters which are capped by a "bare" *pyramidal* nitrogen atom have invariably yielded clusters which have capping imido ligands.[55] It is likewise presumed that a "bare" *pyramidal* nitride ligand is rela-

---

(48) Curtis, M. D.; Klingler, R. J. *J. Organomet. Chem.* **1978**, *161*, 23–37.

(49) Curtis, M. D.; Messerle, L.; Fotinos, N. A.; Gerlach, R. F. *Reactivity of Metal-Metal Bonds*; Chisholm, M. H., Ed.; *ACS Symposium Series* 155; American Chemical Society: Washington, DC, **1981**; pp 221–257.

(50) King, R. B.; Efraty, A.; Douglas, W. M. *J. Organomet. Chem.* **1973**, *60*, 125–137.

(51) King, R. B.; Iqbal, M. Z.; King, A. D., Jr. *J. Organomet. Chem.* **1979**, *171*, 53–63.

(52) Gibson, C. P. Tomchick, D. R.; Dahl, L. F., unpublished observations.

(53) Ginley, D. S.; Wrighton, M. S. *J. Am. Chem. Soc.* **1975**, *97*, 3533–3535.

(54) Smieja, J. A.; Stevens, R. E.; Fjare, D. E.; Gladfelter, W. L. *Inorg. Chem.* **1985**, *24*, 3206–3213.

(55) (a) Bedard, R. L.; Rae, A. D.; Dahl, L. F. *J. Am. Chem. Soc.* **1986**, *108*, 5924–5932. (b) Bedard, R. L.; Dahl, L. F. *J. Am. Chem. Soc.* **1986**, *108*, 5933–5942.

tively unstable[39,55] and is consequently converted to the imido ligand by abstraction of a hydrogen atom from the solvent or adventitious water.

Acknowledgment. Support for this research by the National Science Foundation is gratefully appreciated. Special thanks are due to Dr. A. David Rae for helpful advice in the use of his crystallographic program RAELS, to Dr. Bruce R. Adams for valuable technical assistance in obtaining ^{15}N NMR spectra, and to Mr. Karl C. C. Kharas for a helpful discussion on the applications of electron-counting rules to metal clusters.

Registry No. $1\cdot CH_2Cl_2$, 112068-76-5; 2·hex, 112043-85-3; $Mo_2(\eta^5\text{-}C_5Me_5)_2(CO)_4$, 12132-04-6; $Co(CO)_3NO$, 14096-82-3; Co, 7440-48-4; Mo, 7439-98-7; 1, 112068-75-4; 2, 112459-34-4.

Supplementary Material Available: For each of the two metal clusters, $(\eta^5\text{-}C_5Me_5)_3Mo_3Co_2(CO)_8(\mu_3\text{-}NH)(\mu_4\text{-}N)\cdot CH_2Cl_2$ ($1\cdot CH_2Cl_2$) and $(\eta^5\text{-}C_5Me_5)_2Mo_2Co_3(CO)_{10}(\mu_5\text{-}N)\cdot C_6H_{14}$ (2·hex), tables presented with calculated positions for the hydrogen atoms and with thermal parameters for all atoms (5 pages); listings of observed and calculated structure factor amplitudes for $1\cdot CH_2Cl_2$ and 2·hex (57 pages). Ordering information is given on any current masthead page.

Structure of 2-Lithiophenyl *tert*-Butyl Thioether in Solution and in the Solid State. Detection of Agostic Li–H Interactions by NMR Spectroscopy

W. Bauer,[‡] P. A. A. Klusener,[†] S. Harder,[†] J. A. Kanters,[§] A. J. M. Duisenberg,[§] L. Brandsma,[†]
and P. v. R. Schleyer*[‡]

*Organisch-chemisch Laboratorium, University of Utrecht, Padualaan 8,
NL 3584 CH Utrecht, The Netherlands, Institut für Organische Chemie der Universität Erlangen-Nürnberg,
Henkestr. 42, D-8520 Erlangen, FRG, and Laboratory for Crystal and Structural Chemistry, University of
Utrecht, Padualaan 8, NL-3584 CH Utrecht, The Netherlands*

Received July 20, 1987

tert-Butyl phenyl thioether (**5**) in the presence of *N,N,N′,N′*-tetramethylethylenediamine (TMEDA) is deprotonated with *n*-butyllithium (*n*-BuLi) in hexane to give the ortho lithiation product **6**. X-ray analysis shows **6** to be an endless polymer with dimeric centrosymmetric subunits linked by TMEDA acting as a bridging ligand. The lithiated carbon atom tends toward planar tetracoordination. However, a different structure is present in solution. Structural assignments for **6** in tetrahydrofuran (THF) solution are made by one- and two-dimensional NMR spectroscopy. Complete dissociation into monomers is indicated by ^{13}C NMR (signal multiplicities and ^{13}C, ^{6}Li coupling constants). Close Li–H contacts (detected by ^{6}Li–^{1}H 2D heteronuclear Overhauser spectroscopy, HOESY) are observed for the aromatic hydrogen atom vicinal to the Li substituent and for the *tert*-butyl group. However, TMEDA apparently is not bound to lithium in THF solution.

The lithiation of aromatic compounds often is directed to specific positions by neighboring groups.[1] Ortho lithiation is usually observed when heteroatom substituents, e.g., OR, NR_2, and CH_2NR_2, are present.[2] However, different products are obtained for the pair **1** and **3**: whereas anisole **1** gives ortho metalation (**2**) upon treatment with *n*-BuLi,[3] thioanisole **3** is lithiated at the methyl group to give **4**.[4] However, when the aliphatic substituent

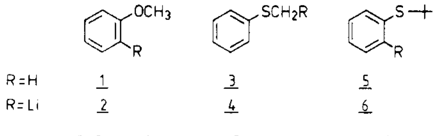

in **3** is replaced by the *tert*-butyl group (which blocks α-lithiation), ortho metalation takes place. The lithiation of *tert*-butyl phenyl thioether (**5**) with *n*-butyllithium (*n*-BuLi) and *N,N,N′,N′*-tetramethylethylenediamine (TMEDA) in hexane was reported by Horner and Lawson.[5] We were interested in comparing the structure of the lithiation product **6** in the solid state and in solution, e.g. with regard to differences in geometry and state of aggregation.

Results and Discussion

Crystals of **6** containing TMEDA were obtained in hexane by deprotonation of **5** with *n*-BuLi.[5] However, as determined by ^{1}H NMR spectroscopy (see below) the TMEDA:**6** ratio in the crystals was 0.5 instead of the 1:1

[†] Organisch-Chemisch Laboratorium, University of Utrecht.

[‡] Universität Erlangen-Nürnberg.

[§] Laboratory for Crystal and Structural Chemistry, University of Utrecht.

(1) (a) Gschwend, H. W.; Rodriguez, H. R. *Org. React.* (*Wiley*) *26*, 1. (b) Beak, P.; Meyers, A. I. *Acc. Chem. Res.* **1986**, *19*, 356.

(2) (a) Narasimhan, N. S.; Mali, R. S. *Synthesis* **1983**, *957*. (b) Posner, G. H.; Canella, K. A. *J. Am. Chem. Soc.* **1985**, *107*, 2571. (c) Beak, P.; Chen, C.-W.; Hunter, J. E.; Kempf, D. J.; Jun, Y.; Wilson, K. D.; Zadjel, W. J. In *Lithium. Current Applications in Science, Medicine, and Technology*; Bach, R. O., Ed.; Wiley: New York, 1985; p 307 ff and references cited therein. (d) Hlasta, D. J.; Bell, M. R. *Tetrahedron Lett.* **1985**, *26*, 2151.

(3) (a) Glaze, W. H.; Ranade, A. C. *J. Org. Chem.* **1971**, *36*, 3331. (b) The X-ray structure of 2-lithioanisole–0.125-tetramethylethylenediamine has recently been solved: Brandsma, L., et al., to be submitted for publication. This structure is quite remarkable as it consists of tetrameric subunits linked by TMEDA analogous to **7**; the subunits are unusual in that sense that two lithium atoms of the Li_4 tetrahedron are complexed by a methoxy group each; one lithium atom is complexed by *two* OCH_3 groups, whereas the remaining Li atom carries the bridging ligand, TMEDA.

(4) Seebach, D.; Gabriel, J.; Hässig, R. *Helv. Chim. Acta* **1984**, *67*, 1083.

(5) Horner, L.; Lawson, A. J.; Simons, G. *Phosphorus Sulphur* **1983**, *12*, 7790 (1983).

0276-7333/88/2307-0552$01.50/0